

Prussian Blue Analogues for CO₂ and SO₂ Capture and Separation Applications

Praveen K. Thallapally,^{*,†} Radha Kishan Motkuri,[†] Carlos A. Fernandez,[†] B. Peter McGrail,[†] and Ghorishi S. Behrooz[‡]

[†]Energy and Environment Directorate, Pacific Northwest National Laboratory, Richland, Washington 99352, and [‡]The Babcock and Wilcox Company, Barberton, Ohio 44203

Received December 3, 2009

Adsorption isotherms of pure gases present in flue gas including CO₂, N₂, SO₂, NO, H₂S, and water were studied using prussian blues of chemical formula M₃[Co(CN)₆]₂ · nH₂O (M = Co, Zn) using an HPVA-100 volumetric gas analyzer and other spectroscopic methods. All the samples were characterized, and the microporous nature of the samples was studied using the BET isotherm. These materials adsorbed 8–10 wt % of CO₂ at room temperature and 1 bar of pressure with heats of adsorption ranging from 200 to 300 Btu/lb of CO₂, which is lower than monoethanolamine (750 Btu/lb of CO₂) at the same mass loading. At high pressures (30 bar and 298 K), these materials adsorbed approximately 20–30 wt % of CO₂, which corresponds to 3 to 5 molecules of CO₂ per formula unit. Similar gas adsorption isotherms for SO₂, H₂S, and NO were collected using a specially constructed volumetric gas analyzer. At close to 1 bar of equilibrium pressure, these materials sorb around 2.5, 2.7, and 1.2 mmol/g of SO₂, H₂S, and NO. In particular, the uptake of SO₂ and H₂S in Co₃[Co(CN)₆]₂ is quite significant since it sorbs around 10 and 4.5 wt % at 0.1 bar of pressure. The stability of prussian blues before and after trace gases was studied using a powder X-ray diffraction instrument, which confirms these materials do not decompose after exposure to trace gases.

Introduction

Hybrid organic–inorganic materials or metal–organic frameworks represent a new class of microporous materials consisting of metal centers linked with organic building blocks to produce a variety of structural frameworks¹ that offer great potential for gas storage,² separation,³ explosive

detection,⁴ catalysis,⁵ and so on.⁶ The conceptual approach for synthesizing these materials is based on the self-assembly of metal centers acting as nodes with organic ligands acting as linkers. As an analogy to zeolite frameworks, this approach to hybrid material construction allows the design of specific nanometer-scale framework geometries with particular pore structures. In contrast to zeolites, for which a relatively limited number of structures exist to date, hybrid materials take advantage of the versatile coordination chemistry, polytopic linkers, which makes it possible to design an almost infinite variety of structures.⁷ Another key advantage is when self-assembly fails during the synthesis with functional linkers, the postfunctionalization of a parent material appears to be a very valuable alternative.⁸ This approach consists of

*To whom correspondence should be addressed. Tel: +1 509 371 7183. Fax: 509 3765368. E-mail: Praveen.Thallapally@pnl.gov.

(1) (a) Wu, C. D.; Hu, A.; Zhang, L.; Lin, W. *J. Am. Chem. Soc.* **2005**, *127*, 8940–1. (b) Thallapally, P. K.; Tian, J.; Kishan, M. R.; Fernandez, C. A.; Dalgarno, S. J.; McGrail, P. B.; Warren, J. E.; Atwood, J. L. *J. Am. Chem. Soc.* **2008**, *130*, 16842–16843. (c) McKinlay, R. M.; Thallapally, P. K.; Atwood, J. L. *Chem. Commun.* **2006**, 2956–2958. (d) Yaghi, O. M.; O’Keeffe, M.; Ockwig, N. W.; Chae, H. K.; Eddaoudi, M.; Kim, J. *Nature* **2003**, *423*, 705–14. (e) Kitaura, R.; Seki, K.; Akiyama, G.; Kitagawa, S. *Angew. Chem., Int. Ed.* **2003**, *42*, 428–430. (f) Dalgarno, S. J.; Thallapally, P. K.; Barbour, L. J.; Atwood, J. L. *Chem. Soc. Rev.* **2007**, *36*, 236–45. (g) Ferey, G.; Mellot-Draznieks, C.; Serre, C.; Millange, F. *Acc. Chem. Res.* **2005**, *38*, 217–25. (h) Zhao, X.; Xiao, B.; Fletcher, A. J.; Thomas, K. M.; Bradshaw, D.; Rosseinsky, M. J. *Science* **2004**, *306*, 1012–1015. (i) Nouar, F.; Eubank, J. F.; Bousquet, T.; Wojtas, L.; Zaworotko, M. J.; Eddaoudi, M. *J. Am. Chem. Soc.* **2008**, *130*, 1833–1835. (j) Zhao, D.; Yuan, D.; Sun, D.; Zhou, H. C. *J. Am. Chem. Soc.* **2009**, *131*, 9186–9188. (k) Ma, S. Q.; Simmons, J. M.; Yuan, D. Q.; Li, J. R.; Weng, W.; Liu, D. J.; Zhou, H. C. *Chem. Commun.* **2009**, 4049–4051. (l) McKinlay, R. M.; Thallapally, P. K.; Cave, G. W. V.; Atwood, J. L. *Angew. Chem., Int. Ed.* **2005**, *44*, 5733–5736.

(2) Yaghi, O. M.; Li, Q. W. *MRS Bull.* **2009**, *34*, 682–690.
(3) (a) Kishan, M. R.; Thallapally, P. K.; Tian, J.; Fernandez, C. A.; Dalgarno, S. J.; Warren, J. E.; Atwood, J. L.; McGrail, B. P. *Chem. Comm* **2010**, 538–540. (b) Bae, Y. S.; Farha, O. K.; Hupp, J. T.; Snurr, R. Q. *J. Mat. Chem.* **2009**, *19*, 2131–2134. (c) Fernandez, C. A.; Thallapally, P. K.; Kishan, M. R.; Nune, S. K.; Sumrak, J. C.; Tian, J.; Liu, J. *Cryst. Growth. Des.* **2010**, DOI: 10.1021/cg9014948.

(4) Lan, A. J.; Li, K. H.; Wu, H. H.; Olson, D. H.; Emge, T. J.; Ki, W.; Hong, M. C.; Li, J. *Angew. Chem., Int. Ed.* **2009**, *48*, 2334–2338.

(5) (a) Lee, J.; Farha, O. K.; Roberts, J.; Scheidt, K. A.; Nguyen, S. T.; Hupp, J. T. *Chem. Soc. Rev.* **2009**, *38*, 1450–1459. (b) Thallapally, P. K.; Motkuri, R. K.; Fernandez, C. A.; Nune, S. K.; Liu, J.; Peden, C. H. F. *Dalton Trans.* **2010**, *39*, 1692–1694.

(6) (a) Doty, F. P.; Bauer, C. A.; Skulan, A. J.; Grant, P. G.; Allendorf, M. D. *Adv. Mater.* **2009**, *21*, 95–101. (b) Czaja, A. U.; Trukhan, N.; Muller, U. *Chem. Soc. Rev.* **2009**, *38*, 1284–1293. (c) Allendorf, M. D.; Bauer, C. A.; Bhakta, R. K.; Houk, R. J. T. *Chem. Soc. Rev.* **2009**, *38*, 1330–1352. (d) Thallapally, P. K.; Dobrzanska, L.; Gingrich, T. R.; Wirsig, T. B.; Barbour, L. J.; Atwood, J. L. *Angew. Chem., Int. Ed.* **2006**, *45*, 6506–6509. (e) Hu, Y. X.; Xiang, S. C.; Zhang, W. W.; Zhang, Z. X.; Wang, L.; Bai, J. F.; Chen, B. L. *Chem. Commun.* **2009**, 7551–7553.

(7) Tranchemontagne, D. J.; Mendoza-Cortes, J. L.; O’Keeffe, M.; Yaghi, O. M. *Chem. Soc. Rev.* **2009**, *38*, 1257–1283.

(8) (a) Wang, Z. Q.; Cohen, S. M. *Chem. Soc. Rev.* **2009**, *38*, 1315–1329. (b) Garibay, S. J.; Wang, Z. Q.; Tanabe, K. K.; Cohen, S. M. *Inorg. Chem.* **2009**, *48*, 7341–7349.

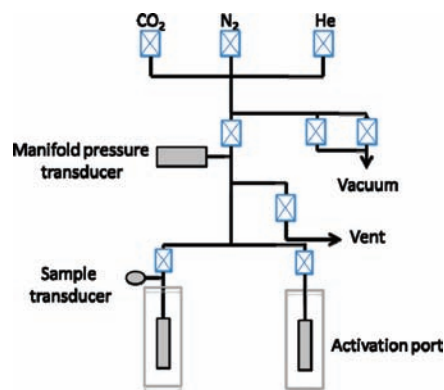
modifying the organic part of the hybrid material with a chemical reaction that takes place within the porous framework.⁹ The adsorption and separation characteristics of these materials can also be modified by systematic selection of the appropriate building blocks.¹⁰ For example, for the isorecticular metal organic framework series, which is based on the hybrid structure, the pore size can be varied from 3.8 Å to 28.8 Å by selecting linkers of various sizes.^{7,10,11} However, closely related metal cyanide complexes or a subclass of metal–organic frameworks called prussian blue analogues have received very little attention. Though prussian blue analogues were discovered in the 17th century, gas adsorption properties of these materials were explored very recently by Long and co-workers, who published a series of papers using these solids for hydrogen storage at 77 K. However, a very limited number of articles were published on CO₂ separation applications using these solids.¹² In this regard, CO₂ capture and removal from a flue gas stream is a technical challenge because of the low concentration of CO₂ (< 15%) present in the gas stream. Alkyl amine solutions are used to scrub the CO₂ from such low concentration streams, and this technology is costly. Therefore, our attention has focused on prussian blue and related microporous materials toward CO₂ capture and separation applications because of a lower energy of regeneration due to the physical adsorption.

Experimental Section

Synthesis of Prussian Blue Analogues. The prussian blue analogues of chemical formula M₃[Co(CN)₆]₂·nH₂O were prepared according to a previously reported procedure.^{12c} Water was distilled and deionized with a Milli-Q filtering system. All other reagents were obtained from Aldrich and were used without further purification, unless otherwise noted. A solution of K₃[Co(CN)₆] (10 mmol in 100 mL of deionized H₂O) was added dropwise to a stirred solution of M(NO₃)₂ (18 mmol in 100 mL of deionized H₂O; M = Co, Zn). The resulting precipitate was allowed to anneal in the mother liquor for 24 h, then was filtered and washed with 3 × 100 mL of deionized H₂O. The precipitate was then dried in air to give Co₃[Co(CN)₆]₂·nH₂O (here onwards, CoCo) and Zn₃[Co(CN)₆]₂·nH₂O (here onwards, ZnCo) in quantitative yield.

Powder X-ray diffraction patterns were collected for compounds CoCo and ZnCo using a Bruker X-ray diffractometer at ambient temperature using Co radiation. BET surface area measurements were performed using a Quantachrome auto-sorb-6 automated gas analyzer at 77 K in the range 1.00 × 10⁻³

Scheme 1. Schematic Diagram of the HPVA-100 Volumetric Gas Analyzer That Was Used to Measure the Adsorption and Desorption Isotherms of CO₂ and N₂



$\leq P/P_0 \leq 1.00$. The surface area was calculated using the widely accepted Brunauer–Emmet–Teller method, and the pore size distribution was determined from the adsorption isotherm by the BJH method.

Differential scanning calorimetry and thermal gravimetric analysis were performed using two different instruments obtained from Setaram and Netzsch. A typical thermal analysis was conducted by heating the sample from room temperature to 500 °C at a heating rate of 2°/min under a nitrogen flow, and the evolved species at different temperatures were characterized using a thermal analyzer coupled with mass spectroscopy. Heats of absorption were calculated using a high pressure calorimetric apparatus obtained from Setaram Instruments. Prior to the heats of absorption, all the samples were activated at high temperatures under a vacuum, and a known amount of CO₂ gas was introduced for enthalpy measurements.

Absorption and desorption isotherms of CO₂ and N₂ at room temperature for CoCo and ZnCo were investigated using an HPVA-100 volumetric gas analyzer. An HPVA-100 volumetric sorption analyzer has been designed to obtain adsorption data at pressures from below atmospheric to 200 bar and at temperatures from cryogenic to 500 °C. Similarly, the uptakes of SO₂, H₂S, and NO were performed using a specially constructed volumetric device for low-pressure experiments. The detailed description of a custom built gas analyzer was discussed elsewhere (see also Scheme 1).¹³

Results and Discussion

Structural Analysis and Characterization. Prussian blue analogues having the chemical formula M₃^{II}[M^{III}(CN)₆]₂·nH₂O (M = transition metals) are constructed from octahedral M^{III}(CN)₆³⁻ complexes which are bridged into a simple cubic lattice by M²⁺ ions (see Figure 1). The defect free three-dimensional cubic lattice was generated by alternating M²⁺ and M³⁺ ions connected through cyanide bridges that are filled with water molecules. The water molecules can be removed at high temperatures under a vacuum to leave the metal cyanide complexes intact. We have successfully synthesized Co₃[Co(CN)₆]₂·nH₂O (CoCo) and Zn₃[Co(CN)₆]₂·nH₂O (ZnCo) as described in the Experimental Section.

Thermal analysis of CoCo and ZnCo shows a sharp weight loss between room temperature and 200 °C that

(9) (a) Ockwig, N. W.; Delgado-Friedrichs, O.; O'Keeffe, M.; Yaghi, O. M. *Acc. Chem. Res.* **2005**, *38*, 176–182. (b) Kitagawa, S.; Uemura, K. *Dynamic Chem. Soc. Rev.* **2005**, *34*, 109–119.

(10) Kitagawa, S.; Kitaura, R.; Noro, S. *Angew. Chem., Int. Ed.* **2004**, *43*, 2334–2375.

(11) (a) Breck, D. W.; Eversole, W. G.; Milton, R. M.; Reed, T. B.; Thomas, T. L. *J. Am. Chem. Soc.* **1956**, *78*, 5963–5971. (b) O'Keeffe, M. *Chem. Soc. Rev.* **2009**, *38*, 1215–1217. (c) O'Keeffe, M. *Nature* **1999**, *400*, 617–618. (d) Eddaoudi, M.; Kim, J.; Rosi, N.; Vodak, D.; Wachter, J.; O'Keeffe, M.; Yaghi, O. M. *Science* **2002**, *295*, 469–472. (e) Delgado-Friedrichs, O.; O'Keeffe, M.; Yaghi, O. M. *Acta Crystallogr., Sect. A* **2006**, *62*, 350–355. (f) Suslick, K. S.; Bhyrappa, P.; Chou, J. H.; Kosal, M. E.; Nakagaki, S.; Smithenry, D. W.; Wilson, S. R. *Acc. Chem. Res.* **2005**, *38*, 283–291. (g) Janiak, C. *Dalton Trans.* **2003**, 2781–2804. (h) Cheetham, A. K.; Ferey, G.; Loiseau, T. *Angew. Chem., Int. Ed.* **1999**, *38*, 3268–3292.

(12) (a) Culp, J. T.; Smith, M. R.; Bittner, E.; Bockrath, B. *J. Am. Chem. Soc.* **2008**, *130*, 12427–12434. (b) Beauvais, L. G.; Long, J. R. *Inorg. Chem.* **2006**, *45*, 236–43. (c) Kaye, S. S.; Long, J. R. *J. Am. Chem. Soc.* **2005**, *127*, 6506–7. (d) Culp, J. T.; Matranga, C.; Smith, M.; Bittner, E. W.; Bockrath, B. *J. Phys. Chem. B* **2006**, *110*, 8325–8328. (e) Sittichai Natesakhawat, J. T. C. *J. Phys. Chem., C* **2007**, *111*, 1055–1060.

(13) Atwood, J. L.; Barbour, L. J.; Thallapally, P. K.; Wirsig, T. B. *Chem. Commun.* **2005**, 51–53.

(14) Mullica, D. F.; Milligan, W. O.; Beall, G. W.; Reeves, W. L. *Acta Crystallogr.* **1978**, *B34*, 3558–3560.

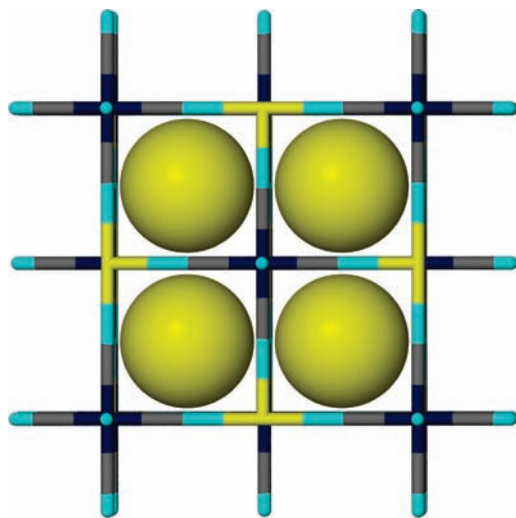


Figure 1. Cubic topology of prussian blue analogues. The coordinates were taken from Mullica et al.¹⁴

corresponds to the loss of water molecules. Around 30% of the weight loss in both the samples corresponds to 10–12 molecules of water per host lattice (Figure 2 and S2 in the Supporting Information (SI)). Powder X-ray diffraction measurements (PXRD) were performed under a vacuum at various temperatures to determine the stability of these frameworks. Identical PXRD patterns were obtained at room and high temperatures indicating that host frameworks remain intact upon removal of trapped water molecules. In order to investigate the microporosity of the synthesized CoCo and ZnCo, BET experiments were conducted using nitrogen adsorption at 77 K. Both samples were calcined at 200 °C for 2 h under a vacuum, and the nitrogen sorption experiments were performed. A typical type I isotherm was observed with a surface area of 712 and 700 m²/g for CoCo and ZnCo, verifying the porous nature of both samples^{1j} (Figure 3 and S3 in the SI). The weight loss and BET surface area of synthesized CoCo and ZnCo were consistent with the results of Long and co-workers.^{12b}

Gas Sorption Analysis. Both the samples were activated overnight at 200 °C under a vacuum, and sorption experiments were performed using an HPVA-100 volumetric gas analyzer. For low pressure experiments, 0.1 bar of CO₂ was dosed into the sample chamber every 10 min, and the volume adsorbed per gram of material was plotted against the pressure. Figure 4 shows the uptake and release of CO₂ at room temperature and 1 bar of pressure. The calculated CO₂ wt % of CoCo and ZnCo at this pressure was found to be 6.7 wt % (1.5 mmol/g) and 7.3 wt % (1.5 mmol/g) with a reversible uptake and release of CO₂ (Figure 4). Similar experiments at high pressure (30 bar) suggest that CoCo and ZnCo sorb 22 wt % (5 mmol/g) and 35 wt % (7 mmol/g) of CO₂, which corresponds to 3 to 5 molecules of CO₂ per formula unit (Figure 4). However, at high pressures, the CO₂ weight percentages in CoCo and ZnCo were very similar to those of the metal–organic frameworks reported thus far but lower than those of the reported MOF-177

(35 mmol/g) and activated carbon (MAXSORB, 25 mmol/g) at the same pressure.^{15,16} No step in adsorption isotherms with CO₂ suggests structural rigidity of CoCo and ZnCo at high pressures; however, several host materials tend to expand and contract during gas uptake and release.^{1b,17} However, in order to envision these materials for postcombustion CO₂ separation applications, it is important to know the effect of other competing gases present in the gas stream; therefore, similar sorption experiments were conducted on N₂, H₂S, SO₂, NO, and water at room temperature.¹⁸ Experiments with nitrogen using the same sample at 1 bar showed sorption of very little or no nitrogen (Figure 4).¹⁹ The selective sorption of CO₂ over N₂ in CoCo and ZnCo can be explained by small pore size and strong dipole–quadrupole interactions between the highly polarizing open-metal sites facing the cavity that can discriminate the gases. These results suggest that these materials can discriminate the gases (CO₂, 3.3 Å; over N₂, 3.64 Å; and H₂, 2.8 Å) which can have significant industrial applications. Therefore, similar gas sorption experiments were conducted on CoCo and ZnCo at room temperature and 1 bar of pressure of SO₂, H₂S, and NO using a custom built volumetric gas analyzer to investigate the selectivity between CO₂ and other trace gases found in a flue gas stream.^{6a,20} At close to 1 bar of equilibrium pressure, CoCo sorbs around 2.5 mmol/g (17 wt %) of SO₂ with slight hysteresis in the desorption, and it sorbs ~2.7 mmol/g (9 wt %) and 1.2 mmol/g (3.6 wt %) of H₂S and NO under a similar equilibrium pressure (Figure 5). In particular, the uptake of SO₂ and H₂S in CoCo is quite significant since it sorbs 10 and 4.5 wt % at 0.1 bar of pressure. Similarly, ZnCo sorbs 1.8 mmol/g (13 wt %) of SO₂ at 1 bar of equilibrium pressure, whereas it sorbs 2.1 mmol/g (8 wt %) of H₂S and 0.1 mmol/g of NO (Figure 6). From these measurements, it is clear that CoCo and ZnCo sorb a range of contaminants at room temperature and moderate pressures, and the uptake of H₂S in particular is in good agreement with the reported MIL-53 and other sorbents.²¹ However, it is important to know the stability of the host framework upon SO₂, H₂S, and NO uptake; therefore, thermogravimetric analyses coupled with mass spectroscopy (TG-MS) and powder X-ray diffraction experiments were conducted on CoCo and ZnCo after each sorption experiment. There is no change in PXRD of CoCo and ZnCo before and after exposure to the above gases, suggesting neither of these gases reacted chemically with the host framework (Figure 7). Similarly, TG-MS analysis after the sorption experiments shows that none of the trapped gases were

(16) Millward, A. R.; Yaghi, O. M. *J. Am. Chem. Soc.* **2005**, *127*, 17998–17999.

(17) Thallapally, P. K.; McGrail, B. P.; Dalgarno, S. J.; Schaefer, H. T.; Tian, J.; Atwood, J. L. *Nat. Mater.* **2008**, *7*, 146–150.

(18) Britt, D.; Tranchemontagne, D.; Yaghi, O. M. *Proc. Natl. Acad. Sci. U.S.A.* **2008**, *105*, 11623–11627.

(19) Chen, B. L.; Ma, S. Q.; Zapata, F.; Fronczek, F. R.; Lobkovsky, E. B.; Zhou, H. C. *Inorg. Chem.* **2007**, *46*, 1233–1236.

(20) (a) Thallapally, P. K.; Dalgarno, S. J.; Atwood, J. L. *J. Am. Chem. Soc.* **2006**, *128*, 15060–15061. (b) Thallapally, P. K.; McGrail, B. P.; Atwood, J. L. *Chem. Commun.* **2007**, 1521–1523. (c) Thallapally, P. K.; McGrail, B. P.; Atwood, J. L.; Gaeta, C.; Tedesco, C.; Neri, P. *Chem. Mater.* **2007**, *19*, 3355–3357.

(21) Hamon, L.; Serre, C.; Devic, T.; Loiseau, T.; Millange, F.; Ferey, G.; De Weireld, G. *J. Am. Chem. Soc.* **2009**, *131*, 8775–8779.

(15) Caskey, S. R.; Wong-Foy, A. G.; Matzger, A. J. *J. Am. Chem. Soc.* **2008**, *130*(33), 10870–10872.

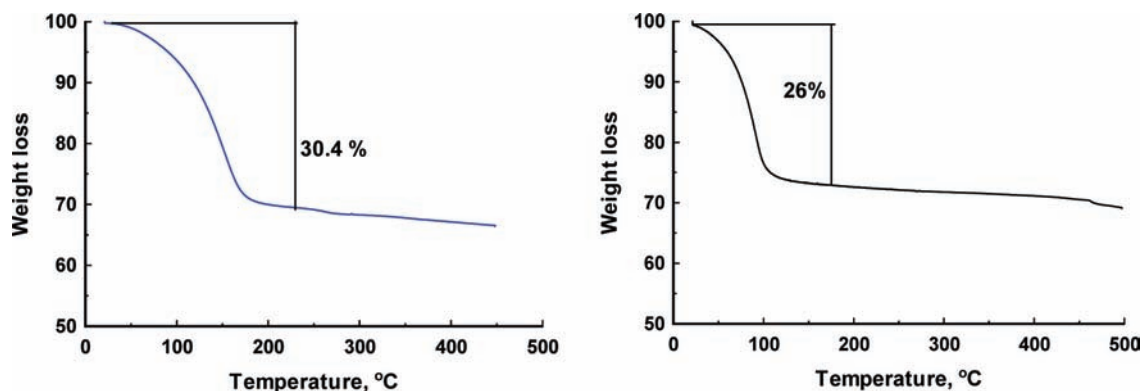


Figure 2. Thermal analysis of CoCo (Left) and ZnCo (Right) between room temperature and 450 °C. Notice that 30% and 26% of the weight loss was due to the loss of solvent water molecules.

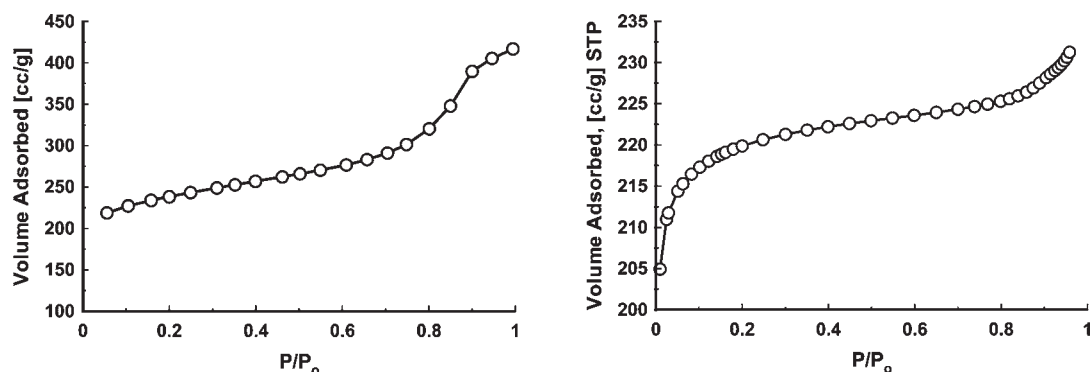


Figure 3. BET surface area of CoCo (Left) and ZnCo (Right) at 77 K and 1 bar of N₂.

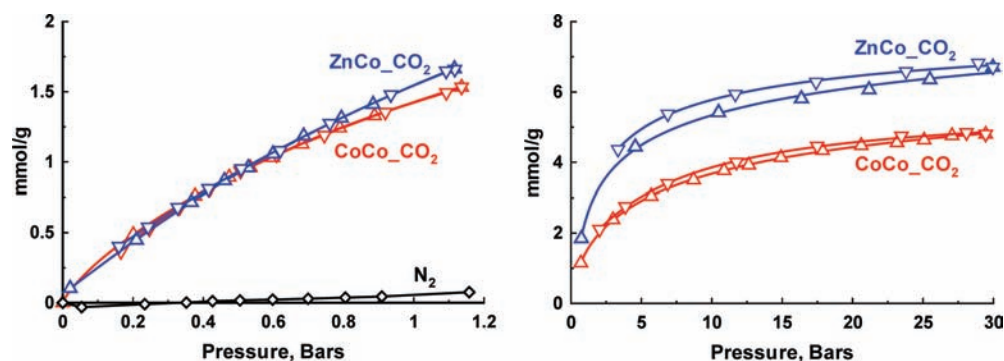


Figure 4. Carbon dioxide adsorption (Δ) and desorption (∇) in CoCo and ZnCo at room temperature and low (left)/high (right) pressure. Notice the selectivity between CO₂ and N₂ at low pressures.

detected using mass spectra, except that traceable peaks for H₂S, NO (CoCo), and water (CoCo and ZnCo) were detected with a weight loss of 3–7% that can be attributed to the loss of water molecules ($m/z = 18$ in mass) that adsorbed during the sample transfer (Figures S4–S5 in the SI).²² The close scrutiny of the TG-MS data of CoCo exposed to H₂S and NO shows the release of H₂S and NO at a slightly higher temperature (~ 70 °C) suggesting the possibility of using these sorbents to capture a range of gases at room temperature and to desorb each gas at different temperatures. To determine whether the impurities in a flue stream will not influence performance, CO₂ uptake was measured post-exposure to impurities. The

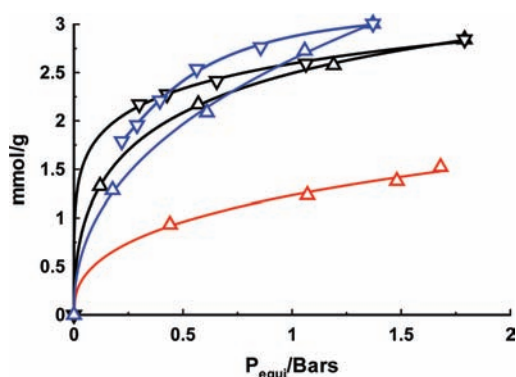


Figure 5. Adsorption (Δ) and desorption (∇) of SO₂ (black), H₂S (blue), and NO (red) using CoCo at room temperature and 2 bar equilibrium pressure. Notice the hysteresis in the desorption of SO₂ and H₂S.

(22) Windisch, C. F.; Thallapally, P. K.; McGrail, B. P. *Spectrochim. Acta, Part A* 2009, 74, 629–634.

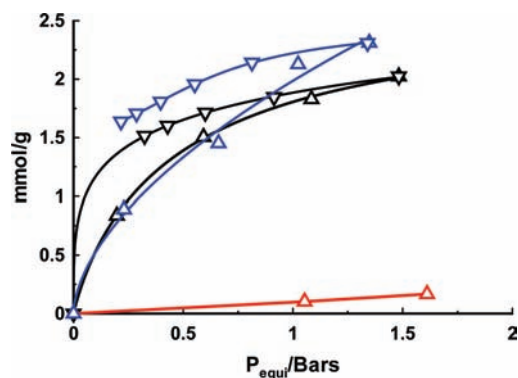


Figure 6. Adsorption (Δ) of SO_2 (black), H_2S (blue), and NO (red) using ZnCo at room temperature. Notice the hysteresis in the desorption (∇) of SO_2 and H_2S .

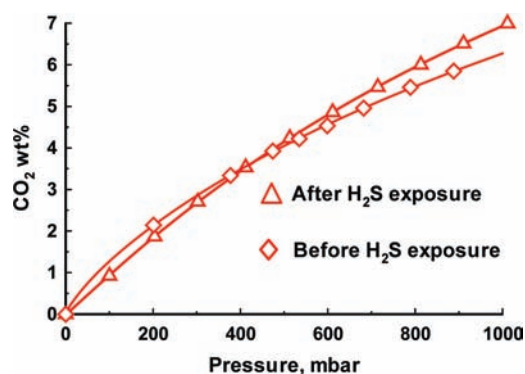


Figure 8. CO_2 uptake at 1 bar and room temperature in CoCo before and after exposure to H_2S . Notice no change in CO_2 weight capacity, suggesting impurities do not have any effect on these sorbents.

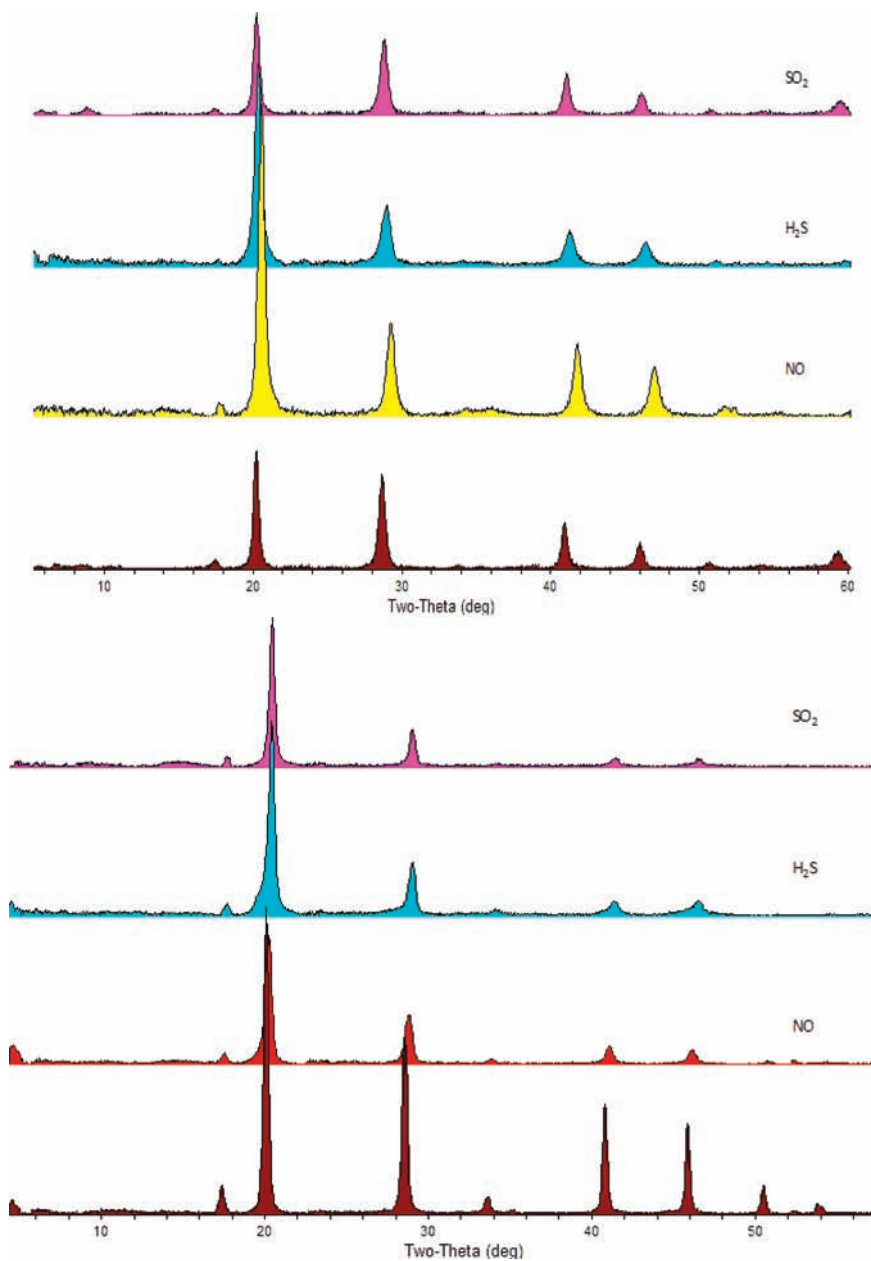


Figure 7. PXRD (Co radiation) of CoCo (top) and ZnCo (bottom) before and after exposure to SO_2 , H_2S , and NO . Notice no change in PXRD is observed.

sample was activated at a high temperature ($150\text{ }^\circ\text{C}$) under a vacuum for several hours to remove all the trace

gases, and sorption experiments using CO_2 as an adsorbate were performed. Figure 8 shows the CO_2 uptake on

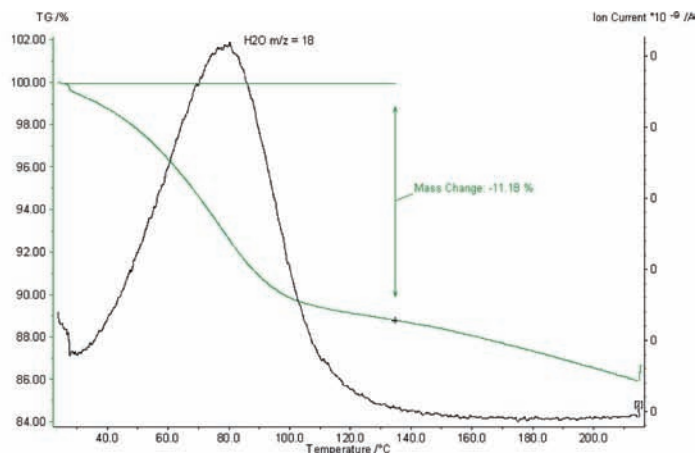
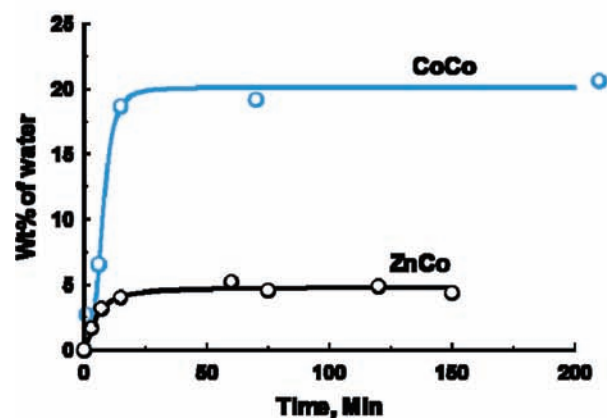


Figure 9. Uptake of water vapor from the air as a function of time with CoCo and ZnCo at room temperature (left). The corresponding TG-MS plot (right) on CoCo exposed to the air suggests a loss of water molecules from the cavity.

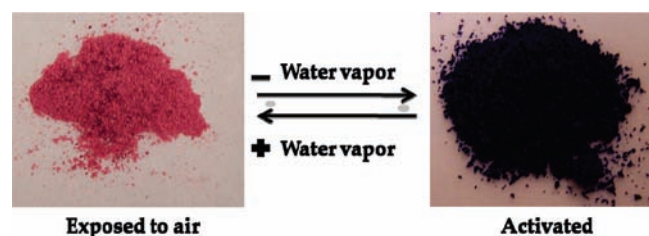


Figure 10. Color changing properties of CoCo upon absorption and desorption of water vapor.

CoCo at 1 bar and room temperature suggesting the impurities have no impact on the performance of these materials.

Along with the absorption kinetics of the pure gases studied above, a large amount of water vapor also exists in a majority of the gas streams. In particular, flue gas contains $\sim 40\%$ water vapor, so it is important to address the absorption and desorption kinetics of water vapor using these sorbents. In this regard, a few milligrams of freshly calcined samples was exposed to air every five minutes and subsequently subjected to TG-MS to observe the weight loss corresponding to the loss of water molecules. The absorption of water as a function of time was shown in Figure 8, which indicates a 20% weight loss within 15 min of exposure in CoCo but only a $< 5\%$ weight loss for ZnCo (Figure 9). However, a similar weight loss (20%) was also observed for ZnCo after exposure for several weeks. The mass corresponding to the m/z 18 clearly indicates the weight loss is due to the release of water molecules (Figure 9 and Figure S6 in the SI). To further support our evidence of water uptake, the crystals of CoCo turn a pink color upon exposure to air due to the charge transfer interactions between the host and water molecules, whereas they become dark blue when trapped water molecules are removed (Figure 10).^{20b} A similar observation was made for ZnCo but not one as remarkable as for CoCo. There is no indication of any color change after the sorption experiments with the above gases, suggesting no strong interaction between the host and guest gas molecules as observed in related materials.^{20b}

Heats of absorption and desorption of the sorbents are critical for economic analysis along with the adsorption and desorption isotherms. Therefore, heats of enthalpy were obtained using a high pressure calorimetric appara-

tus. At room temperature, the enthalpies of CoCo and ZnCo were found to be 6.8 and 7.1 kcal mol⁻¹, which is equivalent to 293 (CoCo) and 253 (ZnCo) Btu/lb of CO₂, which is low compared to 700 Btu/lb in the MEA process with the same weight percentage of CO₂ and is comparable to the reported MOFs and organic solids.^{1h,20c} This suggests the heat needed for CoCo and ZnCo is $\sim 1/3$ that of an existing MEA process (Figure S7 in the SI).

Conclusion

In conclusion, the capture of CO₂ from large industrial power plants or synfuel plants requires a detailed understanding of chemical and physical properties associated with materials that are cheaper in order to achieve a cost of \$5/ton of captured CO₂. There is a critical need for alternative materials for CO₂ capture that possess a high mass capacity, selectivity, and rates of regenerability at an economically viable cost. In depth characterization of ZnCo and CoCo toward CO₂, H₂S, and SO₂ scrubbing application looks very attractive at the moment; however, pure gas adsorption isotherms will not provide the desired information, as the dynamic behavior of the mixture of gases is more important. Therefore, further studies are in progress to access these materials for CO₂ uptake and selectivity in the presence of other trace gases.

Note Added in Proof: In this paper we mentioned that there was no change in the network topology of ZnCo upon adsorption of water. However, we now note that cubic zinc hexacyanocobaltate (ZnCo) transforms into a rhombohedral phase when the coordinated water molecules are removed and then returns to the cubic phase when it is exposed to air containing water vapor. This could explain the results of Figure 9 in our paper and probably also of some of the other figures. It seems that the water adsorption isotherm for Zn shown in Figure 9 corresponds to a mixture of cubic and rhombohedral phases. The inverse structural change, from rhombohedral to cubic requires a relatively large equilibrium time because the Zn is found within a tetrahedral coordination environment.²³

Acknowledgment. This work was initially started under Laboratory Directed Research Development funding and

(23) Krap, C. P.; Zamora, B.; Reguera, L.; Reguera, E. *Microporous Mesoporous Mater.* **2009**, *120*, 414.

later supported by The Babcock and Wilcox Company. The Pacific Northwest National Laboratory is operated by Battelle for the U.S. Department of Energy under Contract DE-AC05-76RL01830.

Note Added after ASAP Publication. This paper was published on the Web on February 18, 2010. A Note Added

in Proof paragraph was added, and the corrected version reposted on April 26, 2010.

Supporting Information Available: Details of CoCo and ZnCo surface area, thermogravimetric analysis, PXRD, and heats of absorption. This material is available free of charge via the Internet at <http://pubs.acs.org>.